Proceedings of the 9th World Congress on Momentum, Heat and Mass Transfer (MHMT'24)
London, United kingdom – April 11 – 13, 2024
Paper No. ENFHT 263
DOI: 10.11159/enfht24.263

A Comparative Experimental Investigation on Charging and Discharging of Paraffin Wax PCM with Surface and Volume Heating Approach

Abhishek Singh Kashyap[1], Vishal Bhalla[2], Himanshu Tyagi[1]
[1]Department of Mechanical Engineering, Indian Institute of Technology Ropar
Rupnagar - 140001, Punjab, India
abhishek.19mez0009@iitrpr.ac.in; himanshu.tyagi@iitrpr.ac.in
[2]Amrita School of Artificial Intelligence, Coimbatore,
Amrita Vishwa Vidyapeetham, 641105, Tamil Nadu, India
b_vishal@cb.amrita.edu

Abstract **-** Solar energy is a promising alternative to fossil fuels for various domestic and industrial thermal applications. However, to deal with its intermittent nature, solar thermal energy storage (STES) is a promising technology for continuous and sustainable operation. This study presents an experimental investigation for the complete charging-discharging cycle of paraffin wax PCM with surface and volume heating. Surface heating has been abbreviated as SH, and volume heating as VH. The comparison in both studies has been made based on temperature rise at the end of the charging process. The SH shows a temperature rise of 67.28 °C, while with the VH, a temperature rise of 59.25 °C is obtained. The effect of variation in heat flux has also been investigated by varying the distance between the light source (halogen lamp) and the receiver (glass beaker filled with paraffin wax). A decrease of 16.01 °C is obtained for the SH when the distance has been increased from 8 to 10 cm. From the results, it is concluded that SH is a more promising approach than VH without the optical properties enhancement of paraffin wax.

Keywords**:** Solar thermal energy storage, Phase change materials, Surface heating, Volume heating, Paraffin wax.

1. Introduction

The importance of solar energy is increasing widely because of its extensive availability and high potential to be converted into thermal energy by using solar collectors [1]. The primary restriction to continuous usage of solar energy is its intermittent availability. To deal with this intermittency, thermal energy storage (TES) is a pivotal technology that stores thermal energy and provides it during high demand. Latent thermal energy storage (LTES) is an attractive technology due to its high-energy storage density and short-to-long term energy storage duration [2]. The solid-liquid phase change materials (PCM) are the medium of LTES, which stores the energy in the form of sensible heat when it is in either the solid or liquid phase and the form of latent heat when the phase changes from solid to liquid during the charging process[3]. PCM is classified as organic, inorganic, and eutectic PCM, and among these three, organic PCMs are lauded due to their excellent thermal and chemical stability, non-toxic behaviour, and high latent heat of fusion. At the same time, the low thermal conductivity has been a demerit of organic PCM [4, 5].

In solar thermal energy storage (STES), integrating solar collectors with LTES units is an active research area with researchers' primary interest in heat transfer enhancement techniques[6, 7]. The integration of solar collectors with the LTES unit can be done by attaching the PCM layer to the absorber plate, incorporating PCM into the water storage tank and integrating the solar collector with a shell-and-tube type PCM storage unit [8]. To enhance the heat transfer within the PCM container, the researchers have adopted various techniques, i.e. incorporation of extended surfaces, metal matrix, encapsulation of PCM, etc. In the conventional integration techniques, the heat is transferred to the PCM by the hot heat transfer fluid (HTF). Conduction and convection are the primary heat transfer mechanisms in these techniques. Recently, researchers have found a way to charge the PCM optically with the photo-thermal effect [9, 10]. In this process, the PCM interacts directly with light and gets heated. During the interaction of light with the PCM, initially, the heat is absorbed in the solid phase, and as soon as the melting temperature of the PCM is reached, the PCM changes its phase from solid to liquid and stores the latent heat. Optical charging becomes an advantageous technology which can be applied to STES as the solar radiation can directly interact with the PCM, which is encapsulated in a container and acts as the thermal storage unit.

Integrating the PCM layer at the bottom of the flat plate collector is advantageous for solar domestic hot water systems [11, 12]. The fins attached to the absorber plate can increase the melting rate of the PCM layer [13]. Incorporation of multi-tubes in the solar collector with the PCM layer at the bottom maintains a high absorber tube temperature during off-sunshine hours [14]. The extended surfaces on the tubes increase the solar collector's heat transfer rate and efficiency [15]. Incorporating the encapsulated PCM inside the water tank is a promising technique to maintain the water temperature near the PCM melting temperature and above ambient temperature [16, 17]. The shell-and-tube heat storage unit consists of two cylindrical pipes in which. One consists of the PCM, and the other carries the working fluid. Incorporating the multi-tubes and fins enhances the melting rate of the PCM [18]. The experimental measurements of the spectral transmittance of the paraffin wax PCM with a melting temperature of 32 °C show that in the solid phase, the transmittance is nearly 5%, and in the liquid phase, the transmittance is almost 90% [19].

The present experimental investigation is focused on the STES with a primary objective to comparing the two cases of charging process of PCM, i.e., VH v/s SH. In VH, the light directly incidents upon PCM, while, In SH of PCM, the light incidents upon a selective surface which is placed on top of the PCM. The investigation is extended to obtain the effect of the heat flux on the temperature variation of PCM by varying the distance (*H*) of the halogen lamp from the beaker.

2. Experimental Setup and Procedure

The experimental setup consists of a light source, a PCM container, a thermocouple, a cooling fan, a data acquisition system (DAQ) and a laptop. The schematic of the experimental setup is presented in Fig. 1 (a). A halogen lamp (make Phillips, Colour temperature – 3400 K) has been taken as the light source, which provides the light on the top of the receiver. The receiver is a glass beaker of 10 ml in which the PCM is filled. A calibrated K-type thermocouple is taken for the temperature measurement connected to DAQ (National Instruments, NI 9213). The thermocouple is placed at the core of the glass beaker, i.e., at the centre of height and radius. The temperature data from the DAQ is fetched to the computer via Lab View software.

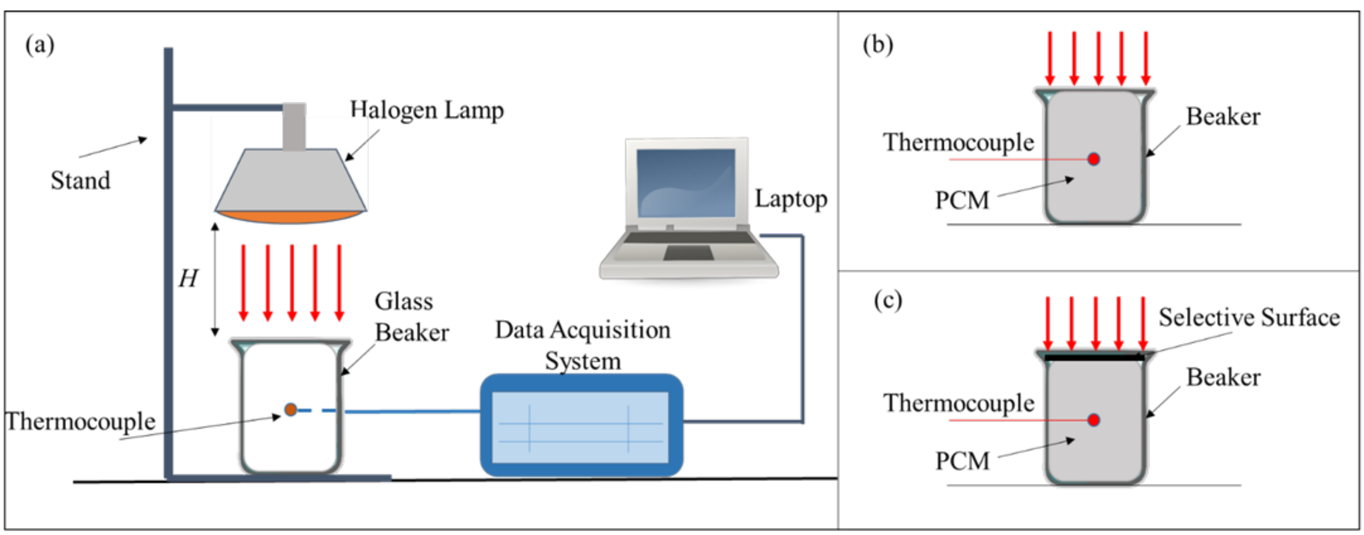

Fig. 1: (a) Schematic of experimental setup (b) Volume heating of PCM (c) Surface heating of PCM.

The experiments have been conducted for 2 cases. Case 1 is the charging of PCM with the VH approach, as shown in Fig. 1 (b). The light from the halogen lamp directly incident upon the PCM (filled inside the glass beaker) and transfers the heat to the depth. Case 2 is the SH approach using a selective surface on the top of the PCM, as shown in Fig. 1 (c). In case 2, the light incident upon the selective surface, which absorbs the heat and transfers it to the PCM through conduction heat transfer phenomena. The experiments for both cases have been performed under similar ambient conditions, i.e., ambient temperature. To obtain the effect of heat flux on the charging process, the distance of the halogen lamp from the beaker (*H*) is varied, i.e., the lower the *H*, the higher is the heat flux and vice versa. The heat flux at both values of *H* is measured with the power meter (Newport, Model 1918-R). At $H = 8$ cm, the heat flux is measured to be 0.75 W/cm^2, and at $H = 10$ cm, the heat flux is obtained as 0.38 W/cm^2. In order to obtain repeatability, all experiments have been conducted 3 times. The uncertainty associated to temperature measurement leads to the statistical error. The error analysis has been done using the student's t-test with 95% confidence level.

For the present experimental investigation, paraffin wax has been taken as the PCM, and the thermophysical properties have been presented in Table 1. The experiments have been performed for a complete charging-discharging cycle. The solid paraffin wax is initially held in a 10 ml beaker at ambient temperature. The Charging (melting) process is carried out for 20 mins, and after that, the halogen lamp is switched off for the discharging (solidification) process in ambient conditions for the next 60 mins. During the charging process, a cooling fan is placed at 6 cm from the halogen lamp as shown in Fig. 1 (a), because the halogen lamp gets heated while providing light to the beaker. The temperature is measured by the calibrated K-type thermocouple, and the recorded data is fetched in the laptop with the help of the DAQ system and Lab view software.

Table 1: Thermophysical properties of paraffin wax [4].

Property	Solid Phase	Liquid Phase
Phase change Temperature (°C)	64	
Latent heat of Fusion (kJ/kg)	173.6	
Thermal Conductivity (W/m·K)	0.346	0.167
Density (kg/m^3)	916	790

3. Results and Discussion

The experimental results for both the cases are presented in the subsections.

3.1. Case 1: Volume Heating (VH) and discharging of PCM

In VH, the top layer of the solid PCM absorbs the light and conducts it through the depth of the beaker, which results in the temperature rise of PCM. As soon as the melting temperature of the PCM is reached, the solid PCM changes its phase into liquid. Fig. 2 shows the temperature variation of PCM v/s time when *H* is 8 cm. The results have been plotted for all three experiments, and a good repeatability without significant error is obtained in the temperature variation. It can be observed that during the charging process the phase change from solid to liquid occurs instantly due to high heat flux available and hence the temperature rises rapidly. At the end of 20 mins, the PCM attains a maximum value of temperature 84.73 °C (at nearly 16 mins), and the temperature starts to remain nearly the same or decreases a little for the rest of the charging duration. The reason behind that is the high transmittance of the liquid paraffin wax, which absorbs very low energy. Simultaneously the light transmits to the solid PCM layer adjacent to the liquid PCM layer. After the end of the charging process at 20 mins, the discharging starts in the ambient conditions for the next 60 mins, and the final temperature reaches to 27.89 °C.

As shown in the graph, the temperature of the liquid PCM starts decreasing rapidly due to the high-temperature difference or thermal potential available. After, the PCM solidifies in the mushy region while changing its phase from liquid to solid. After the complete phase change of liquid paraffin wax into solid, the temperature decreases at a lower rate due to lesser thermal potential availability. It can also be seen from the figure that during melting, the temperature of paraffin wax increases rapidly due to the high heat flux provided to it. Hence, no slope decrement is obtained during the phase change from solid to liquid. On the other hand, during the discharging process, the decrement in the slope of the temperature variation is obtained near the phase change temperature due to relatively lesser thermal potential.

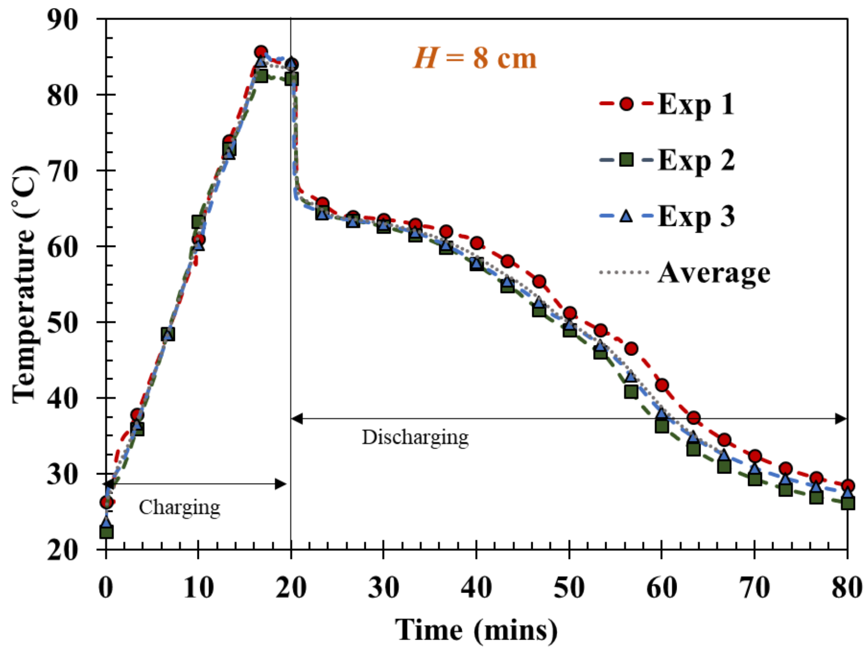

Fig. 2: Temperature variation of PCM for VH and discharging process vs time at *H* = 8cm.

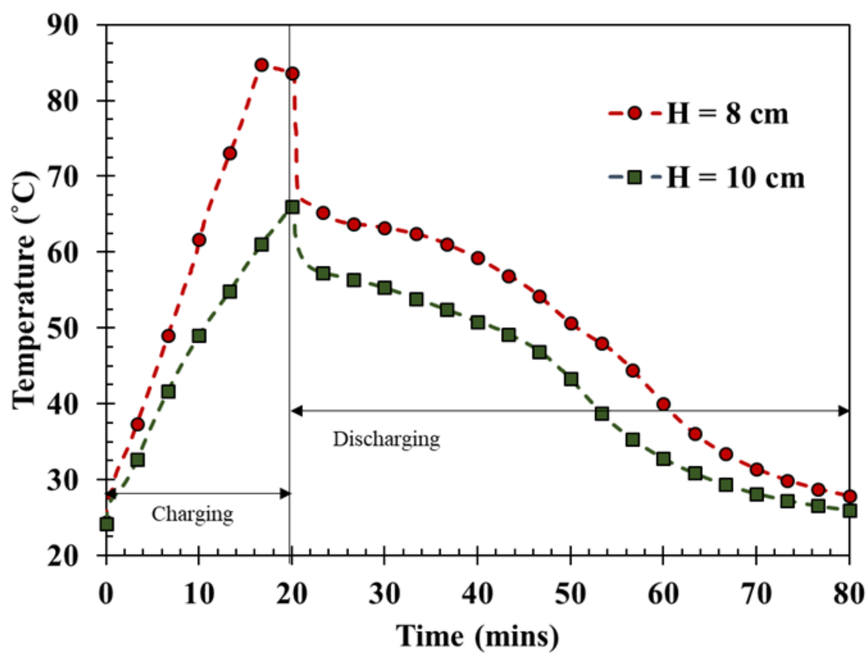

Fig. 3: Temperature variation of PCM for VH and discharging process vs time at *H* = 8 cm and 10 cm.

The effect of varying heat flux has been investigated for two different values of *H*, i.e., 8 cm and 10 cm. The results have been presented in Fig. 3 by taking the average values of the three experiments performed for each value of *H*. It is observed from the figure that at the end of the charging process, the maximum temperature 83.68 °C is obtained for the *H* to be 8 cm because of the highest heat flux provided from the minimum *H*. The minimum temperature 66.06 °C is obtained for the *H* to be 10 cm because of the corresponding minimum heat flux. It can be stated that a decrement of 17.62 °C is obtained while the heat flux is changed from 0.75 W/cm^2 to 0.38 W/cm^2. At the end of the discharging process, the temperature reaches 25.97 °C for *H* to be 10 cm.

3.2. Case 2: Surface heating (SH) and discharging of PCM

In SH, the light from halogen lamp incidents upon the selective surface, which is held to be in proper contact with the PCM. The selective surface absorbs the heat and transfers it to the adjacent layer of PCM via conduction, which results in heat transfer through the depth of the PCM in the beaker. Fig. 4 presents the temperature variation of the PCM v/s time for the distance (H) of 8 cm for all three experiments, and a good agreement between the results can be seen. As the high heat flux is provided, the phase change during charging process is obtained instantly. The average temperature value after 20 mins of charging is 93.58 °C. After the phase change from solid to liquid, the temperature rise phenomenon in SH is different from VH. In SH, the selective coating receives the energy and keeps conducting it to the PCM and hence the temperature keeps increasing. At the end of the discharging process, the average temperature is obtained as 30.72 °C. During the discharging process, initially, the temperature of the PCM drops at a faster rate in liquid phase in comparison to the solid phase due to high thermal potential availability. As in the VH approach, no slope change during the melting of PCM is obtained due to high heat flux provided.

The effect of varying distance (H) has been obtained at two values of H, which are 8 cm and 10 cm. The results have been presented in Fig. 5 by taking average values of the three experiments performed for each value of H. The figure shows that maximum temperature 93.58 °C is obtained at the end of the charging process, for the H = 8 cm, because of the highest heat flux provided from the minimum distance. The minimum temperature of 76.21 °C is obtained for the H = 10 cm corresponding to minimum heat flux. At the end of discharging process, the temperature reaches to 28.84 °C for H = 10 cm.

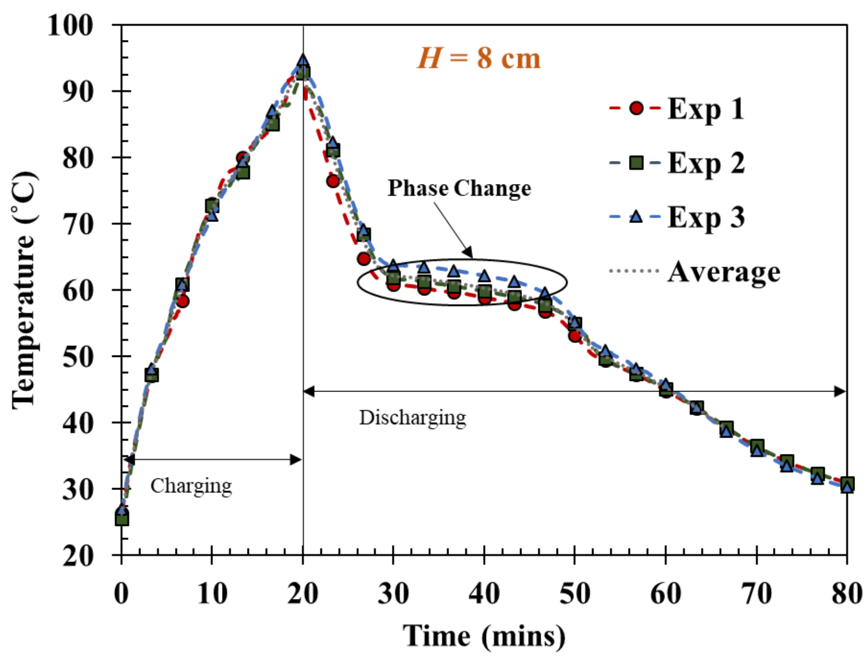

Fig. 4: Temperature variation of PCM for SH and discharging process vs time at H = 8 cm.

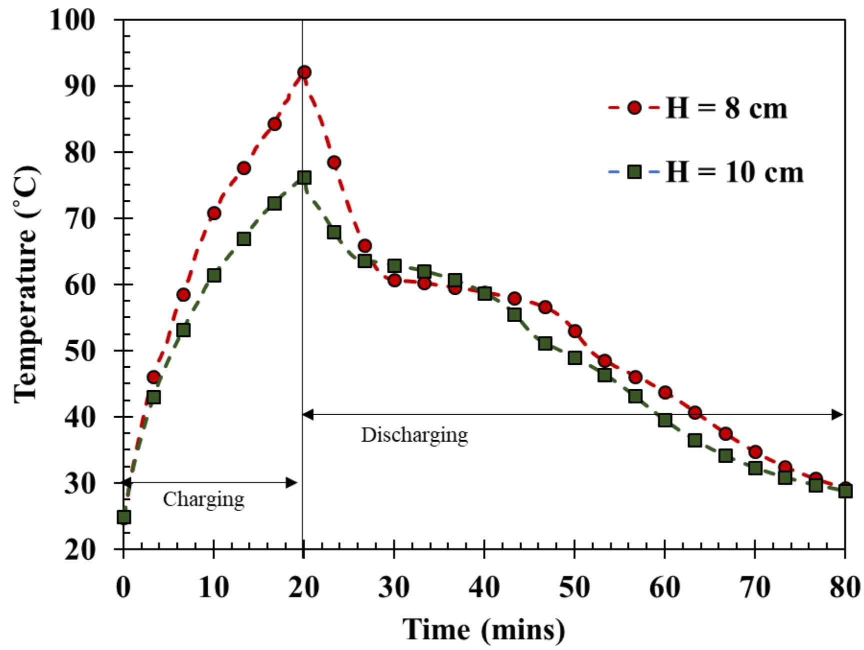

Fig. 5: Temperature variation of PCM for SH and discharging process vs time at H = 8 cm and 10 cm.

3.3. Comparison of VH with SH

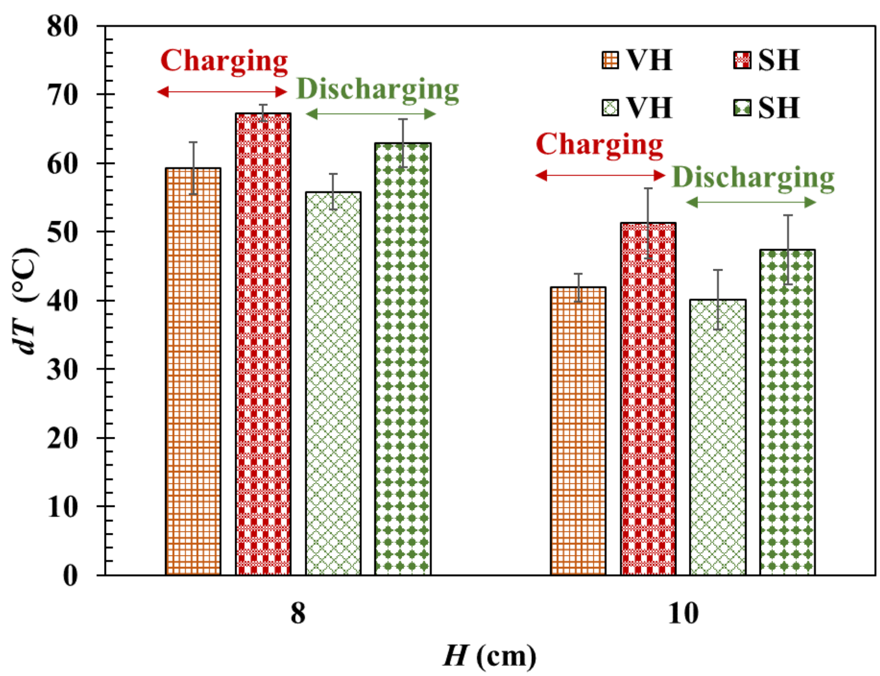

Fig. 6: Temperature difference of PCM for charging and discharging process for both VH and SH at H = 8 cm and 10 cm.

For the charging process, the temperature difference (dT) between the temperature at the end of the charging process (T_{charge}) and the initial temperature ($T_{initial}$) is plotted. For the discharging process, the difference between the T_{charge} and the temperature at the end of discharging charging process (T_{final}) is plotted as the bar graph for both VH and SH approaches. For the charging process, it can be seen from the figure that for both the values of H, a higher temperature difference is obtained for SH to VH. The maximum temperature difference of 67.28 °C is obtained with SH for H = 8 cm, and the minimum temperature difference of 41.88 °C is obtained with VH for H = 10cm. Similarly, for the discharging process, it can be seen from the figure that for both the values of H, a higher temperature difference is obtained for SH in comparison of VH. The maximum temperature difference of 62.86 °C is obtained with SH for H = 8 cm, and minimum temperature difference of 41.1 °C is obtained with VH for H = 10 cm. beaker. In the context of error analysis, the errors associated with all the results have been shown in the bar graph. The result with minimum error of 1.13 °C is obtained for SH with H = 8 cm while the maximum error of 5.1 °C is obtained for SH with H = 10 cm.

4. Conclusion

The present experimental investigation has been conducted to compare the charging of paraffin wax with VH and SH approaches. The temperature change at the core of the receiver (beaker filled with paraffin wax) is obtained to compare both cases while providing the light from a source (halogen lamp). The effect of varying heat flux has been investigated by adjusting the distance of the halogen lamp from the beaker. From the results, it is observed that with SH, a higher temperature at the end of the charging process is obtained compared to the VH approach. A maximum temperature rise of 67.28 °C is obtained for the SH with H = 8 cm, which is 8.02 °C higher than the VH. Increasing the value of H results in lesser heat flux, and hence, lesser temperature rise is obtained with H = 10 cm. For the SH, a decrease of 16.01 °C is obtained while changing the H from 8 cm to 10 cm. The study concludes that without enhancing the optical properties of paraffin wax, SH is a more promising approach than VH for STES.

Acknowledgements

A.S.K. and H.T. thankfully acknowledge the support provided by the Department of Mechanical Engineering at Indian Institute of Technology Ropar.

References

[1] S. A. Kalogirou, "Solar thermal collectors and applications," *Prog. Energy Combust. Sci.*, vol. 30, no. 3, pp. 231–295, 2004, doi: 10.1016/j.pecs.2004.02.001.

[2] International Energy Agency, "Technology Roadmap - Energy Storage," 2014.

[3] I. Dincer and M. A. Ezan, *Heat Storage: A Unique Solution For Energy Systems*. in Green Energy and Technology. Cham: Springer International Publishing, 2018. doi: 10.1007/978-3-319-91893-8.

[4] H. Zalba, B., Marın, J. M., Cabeza, L. F., & Mehling, "Review on thermal energy storage with phase change: materials, heat transfer analysis and applications," *Appl. Therm. Eng.*, vol. 23(3), 251, pp. 251–283, 2003.

[5] A. Sharma, V. V. Tyagi, C. R. Chen, and D. Buddhi, "Review on thermal energy storage with phase change materials and applications," *Renew. Sustain. Energy Rev.*, vol. 13, no. 2, pp. 318–345, 2009, doi: 10.1016/j.rser.2007.10.005.

[6] M. E. Zayed, J. Zhao, W. Li, A. H. Elsheikh, A. M. Elbanna, L. Jing, and A. E. Geweda, "Recent progress in phase change materials storage containers: Geometries, design considerations and heat transfer improvement methods," *J. Energy Storage*, vol. 30, no. January, p. 101341, 2020, doi: 10.1016/j.est.2020.101341.

[7] E. Douvi, C. Pagkalos, G. Dogkas, M. K. Koukou, V. N. Stathopoulos, Y. Caouris, and M. G. Vrachopoulos, "Phase change materials in solar domestic hot water systems: A review," *Int. J. Thermofluids*, vol. 10, p. 100075, 2021, doi: 10.1016/j.ijft.2021.100075.

[8] S. Kee, Yiing, Y. Munusamy, and K. Ong, Seng, "Review of solar water heaters incorporating solid-liquid organic phase change materials as thermal storage," *Appl. Therm. Eng.*, vol. 131, pp. 455–471, 2018, doi: 10.1016/j.applthermaleng.2017.12.032.

[9] J. Liu, L. Chen, X. Fang, and Z. Zhang, "Preparation of graphite nanoparticles-modified phase change microcapsules and their dispersed slurry for direct absorption solar collectors," *Sol. Energy Mater. Sol. Cells*, vol. 159, pp. 159–166, 2017, doi: 10.1016/j.solmat.2016.09.020.

[10] Z. Wang, J. Qu, R. Zhang, X. Han, and J. Wu, "Photo-thermal performance evaluation on MWCNTs-dispersed microencapsulated PCM slurries for direct absorption solar collectors," *J. Energy Storage*, vol. 26, no. March, p. 100793, 2019, doi: 10.1016/j.est.2019.100793.

[11] J. Prakash, H. P. Garg, and G. Datta, "A solar water heater with a built-in latent heat storage," *Energy Convers. Manag.*, vol. 25, no. 1, pp. 51–56, 1985, doi: 10.1016/0196-8904(85)90069-X.

[12] B. M. Y. Rabin, Bar-Niv, E. Kovin, "1995 Rabin - Integrated SCSS based on salt hydrate PCM.pdf." 1995.

[13] K. S. Reddy, "Thermal modeling of PCM-based solar integrated collector storage water heating system," *J. Sol. Energy Eng. Trans. ASME*, vol. 129, no. 4, pp. 458–464, 2007, doi: 10.1115/1.2770753.

[14] A. J. N. Khalifa, K. H. Suffer, and M. S. Mahmoud, "A storage domestic solar hot water system with a back layer of phase change material," *Exp. Therm. Fluid Sci.*, vol. 44, pp. 174–181, 2013, doi: 10.1016/j.expthermflusci.2012.05.017.

[15] H. H. Al-Kayiem and S. C. Lin, "Performance evaluation of a solar water heater integrated with a PCM nanocomposite TES at various inclinations," *Sol. Energy*, vol. 109, no. 1, pp. 82–92, 2014, doi: 10.1016/j.solener.2014.08.021.

[16] M. Mazman, L. F. Cabeza, H. Mehling, M. Nogues, H. Evliya, and H. Ö. Paksoy, "Utilization of phase change materials in solar domestic hot water systems," *Renew. Energy*, vol. 34, no. 6, pp. 1639–1643, 2009, doi: 10.1016/j.renene.2008.10.016.

[17] I. Al-Hinti, A. Al-Ghandoor, A. Maaly, I. Abu Naqeera, Z. Al-Khateeb, and O. Al-Sheikh, "Experimental investigation on the use of water-phase change material storage in conventional solar water heating systems," *Energy Convers. Manag.*, vol. 51, no. 8, pp. 1735–1740, 2010, doi: 10.1016/j.enconman.2009.08.038.

[18] A. Shinde, S. Arpit, P. Km, P. V. C. Rao, and S. K. Saha, "Heat Transfer Characterization and Optimization of Latent Heat Thermal Storage System Using Fins for Medium Temperature Solar Applications," *J. Sol. Energy Eng. Trans. ASME*, vol. 139, no. 3, pp. 1–10, 2017, doi: 10.1115/1.4035517.

[19] D. Zhao, G. Zhang, X. Zhang, and D. Li, "Optical properties of paraffin at temperature range from 40 to 80 °C," *Optik (Stuttg).*, vol. 157, pp. 184–189, 2018, doi: 10.1016/j.ijleo.2017.11.093.